Eur. Phys. J. A **12**, 327–334 (2001)

THE EUROPEAN PHYSICAL JOURNAL A

^{16}O-^{8}Be break-up states and cluster structure of ^{24}Mg

A. Tumino[1,2,a], M. Lattuada[1,3,b], S. Romano[1,3], C. Spitaleri[1,4], D. Vinciguerra[1,3], Z. Basrak[5], O.Yu. Goryunov[6], V.V. Ostashko[6], S. Szilner[5], P. Figuera[1], D. Lo Presti[3,7], C. Petta[3,7], N. Randazzo[3,7], S. Reito[7], G.V. Russo[3,7], and S. Tudisco[1,3]

[1] Istituto Nazionale di Fisica Nucleare, Laboratori Nazionali del Sud, Catania, Italy
[2] Hahn-Meitner-Institut GmbH, Berlin, Germany
[3] Dipartimento di Fisica e Astronomia, Università di Catania, Catania, Italy
[4] Dipartimento di Metodologie Fisiche e Chimiche per l'Ingegneria, Università di Catania, Catania, Italy
[5] Institut Rudjer Boškovic, Zagreb, Croatia
[6] Institute for Nuclear Research, Kiev, Ukraine
[7] Istituto Nazionale di Fisica Nucleare, Sezione di Catania, Catania, Italy

Received: 6 July 2001 / Revised version: 30 August 2001
Communicated by D. Guerreau

Abstract. High-spin states of ^{24}Mg produced in the $^{16}\mathrm{O} + ^{12}\mathrm{C}$ interaction and decaying into the $^{16}\mathrm{O}_{\mathrm{g.s.}} + ^{8}\mathrm{Be}_{\mathrm{g.s.}}$ channel have been observed in the excitation region between 35 and 52 MeV. Spins have been assigned on the basis of the analysis of the measured angular correlations. Some of these states with positive parity correspond to the known resonances of the $^{12}\mathrm{C}(^{12}\mathrm{C},^{8}\mathrm{Be}_{\mathrm{g.s.}})^{16}\mathrm{O}$ reaction belonging to the ^{16}O-2α rotational band of ^{24}Mg. Moreover other resonances show up at higher excitation energy with an energy-spin relationship again suggesting a ^{16}O-2α cluster structure for the associated configuration.

PACS. 25.70.Ef Resonances – 21.60.Gx Cluster models – 24.10.-i Nuclear-reaction models and methods

1 Introduction

The high-energy region of the ^{24}Mg excitation spectrum has recently showed interesting features that have been related to the description of this nucleus in terms of constituent α-particles and/or aggregates of α-particles. At the beginning of the 90's [1] an unusually large ($\Gamma \approx 5$ MeV) structure was found in the $^{12}\mathrm{C} + ^{12}\mathrm{C} \rightarrow ^{12}\mathrm{C}(0_2^+) + ^{12}\mathrm{C}(0_2^+)$ excitation function, corresponding to a resonance at 46.4 MeV in ^{24}Mg. The tentative association of this resonance with a very stretched configuration of six α-particles in a line suggested the need for further investigation and triggered a number of experiments in this direction. The high excitation region of ^{24}Mg was investigated looking at the excitation functions of several exit channels of the $^{12}\mathrm{C} + ^{12}\mathrm{C}$ interaction, for example inelastic scattering and transfer followed by multiple alpha emission [2–7]. A large amount of information was then deduced from these experiments which, on one side, did not allow for any definite conclusion on the association of the 46.4 MeV resonance with the 6α linear chain. On the other hand, new data on high-lying states of ^{24}Mg were made available, which could be associated with different arrangements of the constituent α-particles, as predicted by cluster models.

A conjecture from these measurements was then made [8] concerning the existence in this ^{24}Mg excitation region of at least two types of states populated in the $^{12}\mathrm{C} + ^{12}\mathrm{C}$ interaction. A highly deformed 6α-cluster structure was attributed to one type, leading to final states where both the nuclei are excited above the α-particle decay threshold. The other type was characterised by a smaller degree of deformation, thus feeding outgoing channels below this threshold.

The excitation function of the $^{12}\mathrm{C}(^{12}\mathrm{C}, ^{8}\mathrm{Be}_{\mathrm{g.s.}})^{16}\mathrm{O}_{\mathrm{g.s.}}$ reaction [9,10] showed in fact the presence of several resonant structures in the range $E_{\mathrm{cm}} = 20$ to 36 MeV. The angular distributions measured at the peak energies allowed for spin assignment to each resonance and a linear dependence of E_{cm} *vs.* $J_*(J+1)$ was found. The slope coefficient of about 90 keV, obtained by fitting these data together with data at lower energies reported in the literature, turned out to be consistent with the moment of inertia of the $^{8}\mathrm{Be}_{\mathrm{g.s.}}$-$^{16}\mathrm{O}_{\mathrm{g.s.}}$ system in the rigid rotor approximation. Such states were then associated with the so-called $D1$ configuration of ^{24}Mg, described in the Cranked Cluster Model [11] as a rotating system made of a $^{16}\mathrm{O}_{\mathrm{g.s.}}$ core plus two α-particles.

[a] Alexander von Humboldt Fellow.
[b] e-mail: lattuada@lns.infn.it
Permanent address: Laboratori Nazionali del Sud – INFN, Via S. Sofia 44, I-95123 Catania, Italy.

In order to test the hypothesis of existence of different structured states, a systematic study of a large number of reactions over a wide range of excitation energy is required. This would allow also to inspect how entrance channel effects might interfere in the formation of cluster configurations.

An alternative way of studying highly excited nuclear states consists in looking at the break-up of intermediate systems formed in sequential three-body reactions. In particular, the advantage of this last method lies in the possibility of exploring an extended excitation energy range, with a single beam energy. This technique was applied in the $^{16}O + ^{12}C$ reaction to study the $^{16}O + ^{8}Be$ decay of ^{24}Mg states up to about 35 MeV of excitation energy [12].

Here we report on a recent experiment performed on the $^{16}O + ^{12}C$ reaction, aimed at the extension of the study of ^{24}Mg and ^{16}O states at higher energy decaying into α-particles and/or subsystems of α-particles. In the present paper the results obtained by looking at the $^{8}Be_{g.s.}$-$^{16}O_{g.s.}$ break-up channel of ^{24}Mg will be shown and new information concerning the emitting states at very high excitation energy will be discussed.

2 The experiment

The experiment was performed at the Laboratori Nazionali del Sud in Catania, by using a ^{16}O beam accelerated to 109 MeV by the SMP Tandem and delivered onto a natural-carbon target. Special care was taken in beam collimation in order to produce a beam spot on the target smaller than 1 mm. The detection set-up consisted of two different systems, placed on opposite sides with respect to the beam direction. On one side a telescope, consisting of a 50×10 mm^2, 1 mm thick, silicon Position Sensitive Detector (PSD) and an Ionisation Chamber (IC) in front of them, allowed for detection and identification of charged products in the in-plane angular range of 25° to 35°. Four arrays, each one consisting of a set of twelve 50×4 mm^2, 0.8 mm thick, silicon PSD, covered the polar angular range of 20° to 60° on the other side of the beam. These arrays, later on called ASPEDs (Array of Silicon Position Energy Detectors), were mounted symmetrically with respect to the horizontal plane in such a way to cover an out-of-plane angular range between –6° and 6°.

All detectors were sensitive to the position of the particle along the horizontal dimension and thus were able to give information on the polar angle of emission. An indication of the out-of-plane angle of the particle detected in an ASPED is given by the position of the fired detector in the array. Standard NIM electronic chains were used to process the signals from the IC + PSD telescope. The ASPED read-out was realised by means of front-end electronic boards. Signals were preamplified and shaped through a full custom chip OSCAR [13] and further amplified by operational amplifiers. In order to fit the characteristics of this kind of detectors, the chip OSCAR was specially designed using CMOS technique. Thanks to the advantage of VLSI technique and to the dedicated design, OSCAR has shown good performances in terms of noise and linearity.

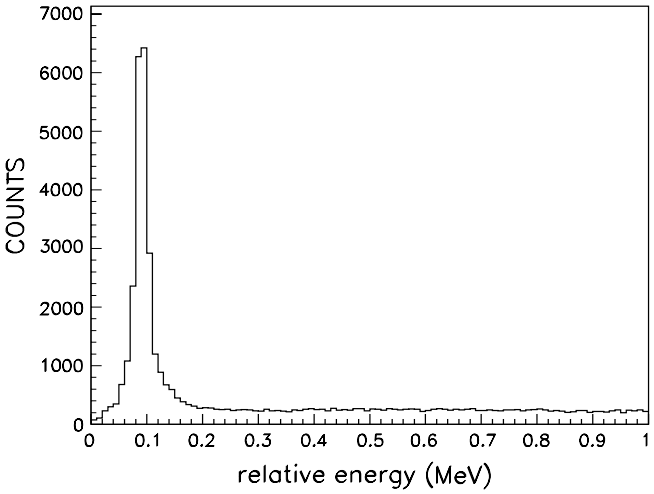

Fig. 1. Relative-energy spectrum of two particles detected in coincidence in the ASPEDs. The peak at 90 keV is due to the 2α decay of $^{8}Be_{g.s.}$.

The trigger for the event acquisition was given by the coincidence of a signal from the PSD + IC system and at least another one from one detector of the arrays. Energy and position informations were stored together with the delay between the time signals for each coincidence event.

3 Data analysis and results

Events were selected according to the number of fired detectors and analysed separately. Energy and position calibration of all the PSDs was performed using the data acquired in preliminary runs of the $^{12}C(^{12}C,\alpha)^{20}Ne$ reaction at several beam energies, after identification of the many α peaks due to excitation of ^{20}Ne states. Data for calibration were taken placing grids with vertical slits in front of the detectors.

For the ASPED calibration, a new method was developed [14] which provides simultaneously energy and position values from the combination of the two signals collected at both edges of each detector.

For the purpose of the present paper we will refer only to the analysis of events due to coincidences between an oxygen ion identified in the telescope and two unidentified particles hitting the arrays.

Assuming equal masses for the two particles detected in the ASPEDs, their relative-energy spectrum was built. Here, the peak around 100 keV indicates the dominant emission of two α-particles emitted from a ^{8}Be nucleus in its ground state (fig. 1). Thus, the $^{16}O + ^{8}Be_{g.s.} + \alpha$ exit channel is fully identified when events falling into the oxygen locus of the $\Delta E - E$ telescope matrix (fig. 2) are selected in coincidence with the events in the $^{8}Be_{g.s.}$ peak. The kinematics were reconstructed under the hypothesis of mass 16 for the oxygen ions, leading to the Q-value spectrum reported in fig. 3. Besides the small background

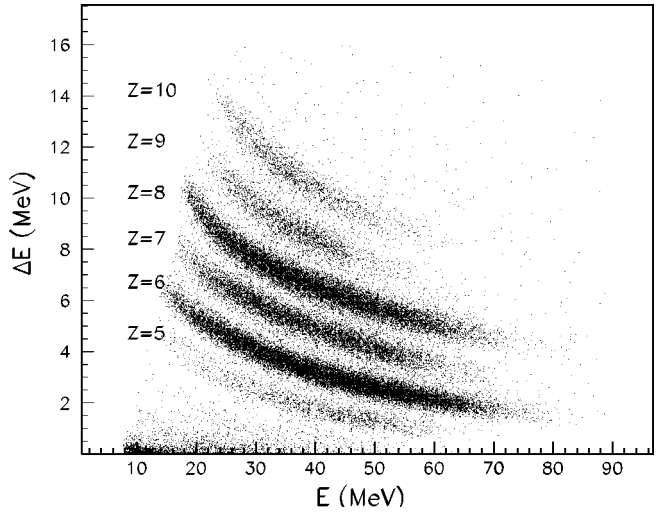

Fig. 2. Typical $\Delta E - E$ spectrum obtained in the $^{16}\mathrm{O} + {}^{12}\mathrm{C}$ interaction.

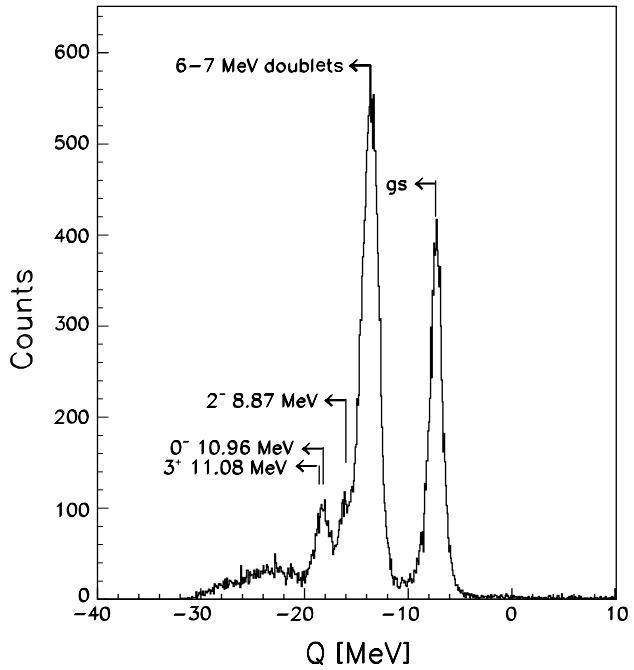

Fig. 3. Q spectrum obtained from the coincidence detection of a ^{16}O nucleus with two unidentified particles, whose mass was assumed to be 4.

mainly due to the residual ambiguity in particle identification, the spectrum is dominated by the peaks due to excitation of particle-stable states of ^{16}O.

The identified ^{16}O nuclei are mainly in the ground state or excited to the first two unresolved doublets of states at around 6 and 7 MeV, respectively, lying under the particle decay threshold.

The small peaks at more negative Q-values were associated with the low-lying unnatural parity states of ^{16}O at 8.87 (0^-) and 10.96–11.08 (2^- and 3^+, respectively) MeV, whose particle decay is prevented by the parity conservation law.

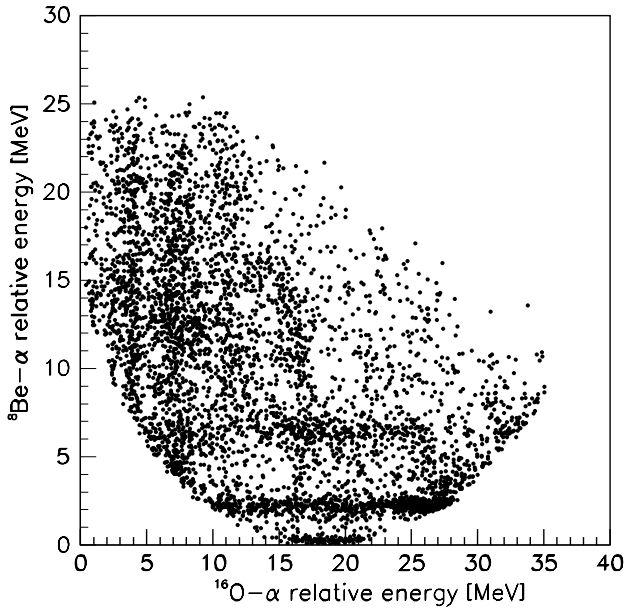

Fig. 4. $^{8}\mathrm{Be}_{\mathrm{g.s.}}$-$\alpha$ relative energy *vs.* $^{16}\mathrm{O}_{\mathrm{g.s.}}$-$\alpha$ relative-energy plot. The horizontal and vertical loci correspond to ^{12}C and ^{20}Ne excited states respectively, and diagonal loci correspond to ^{24}Mg excited states.

The events involving ^{16}O nuclei excited to the two doublet states were not accounted for in the present analysis since the mixing of different spins and parities would prevent any unambiguous characterisation of the emitting ^{24}Mg states. Thus, the analysis was performed by gating on the ^{16}O ground-state peak in the Q-value spectrum.

The $^{16}\mathrm{O}_{\mathrm{g.s.}} + {}^{8}\mathrm{Be}_{\mathrm{g.s.}} + \alpha$ final state can result from a number of different processes including the decay of ^{20}Ne excited states into $^{16}\mathrm{O}_{\mathrm{g.s.}} + \alpha$, ^{12}C excited states into $^{8}\mathrm{Be}_{\mathrm{g.s.}} + \alpha$ or ^{24}Mg states into $^{16}\mathrm{O}_{\mathrm{g.s.}}$-$^{8}\mathrm{Be}_{\mathrm{g.s.}}$ nuclei. Relative energies for any two of the three final particles were then calculated in order to look for possible excitations of their respective intermediate systems. Figure 4 shows the selected events plotted on the $^{8}\mathrm{Be}_{\mathrm{g.s.}} + \alpha$ relative energy *vs.* $^{16}\mathrm{O}_{\mathrm{g.s.}} + \alpha$ relative-energy plane. This representation shows both horizontal and vertical loci, associated with peaks at excitation energies of 7.7, 9.7 and 13.9 MeV in ^{12}C (horizontal loci) and 8.7, 11.9, 15.9 and 21.1 MeV in ^{20}Ne (vertical loci). The peaks in ^{12}C may be associated with its states at $7.65(0^+)$, $9.63(3^-)$ and $14.1(4^+)$ MeV, and in ^{20}Ne with its states at $8.77(6^+)$, $11.95(8^+)$, $15.87(8^+)$ and $21.06(9^-)$ MeV, previously observed in this reaction [15,16]. There is a weak evidence of some diagonal loci crossing those associated with ^{20}Ne states, which may be attributed to high-lying states in ^{24}Mg decaying into the $^{16}\mathrm{O}_{\mathrm{g.s.}}$-$^{8}\mathrm{Be}_{\mathrm{g.s.}}$ final state.

Data were projected on the $^{16}\mathrm{O}_{\mathrm{g.s.}}$-$^{8}\mathrm{Be}_{\mathrm{g.s.}}$ relative-energy axis after selectively removing the background due to $^{12}\mathrm{C}(^{16}\mathrm{O},{}^{16}\mathrm{O}_{\mathrm{g.s.}})^{12}\mathrm{C}^*$ reactions. The $^{16}\mathrm{O}_{\mathrm{g.s.}}$-$^{8}\mathrm{Be}_{\mathrm{g.s.}}$ relative-energy spectrum so obtained is shown in fig. 5a. The ^{24}Mg excitation energy ($^{16}\mathrm{O}_{\mathrm{g.s.}}$-$^{8}\mathrm{Be}_{\mathrm{g.s.}}$ relative energy + 14.1 MeV) is reported in the upper horizontal axis.

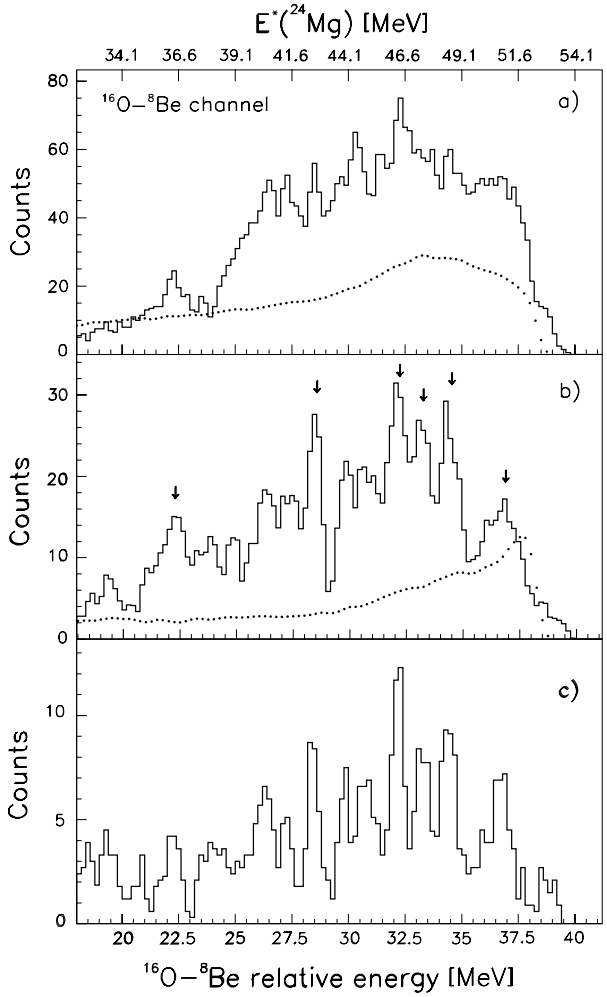

Fig. 5. $^{16}O_{g.s.}$-$^{8}Be_{g.s.}$ relative-energy spectra. a) contains the coincidence data after removing the background due to the $^{12}C(^{16}O,^{16}O_{g.s.})^{12}C^*$ reactions; b) is obtained by making also the in-plane data selection; c) is obtained by further excluding the contribution from contaminant decays of $^{20}Ne^*$. ^{24}Mg excitation energy is reported in the upper horizontal axis.

Several peaks appear indicating the formation of a highly excited $^{24}Mg^*$ intermediate system, which decays into the $^{16}O_{g.s.} + {}^{8}Be_{g.s.}$ channel. A large background is still present, mainly due to $^{20}Ne^* + {}^{8}Be_{g.s.}$ channels. As shown in fig. 4, their contribution is strongly mixed with the process of interest, in a way which makes difficult a selective separation in the spectrum.

However, the process under study, which consists in a first-step emission of the $^{24}Mg^* + \alpha$ system, should be very sensitive to the stretch condition [17], which forces the relative angular momentum between $^{24}Mg^*$and α to be aligned or anti-aligned with the $^{24}Mg^*$ intrinsic spin. As known, this coupling appears to be the most probable for transfer reactions populating final states at high excitation energy. Therefore, ^{16}O and ^{8}Be, coming from the decay of high-lying states in $^{24}Mg^*$, are preferentially coplanar with the first emitted α-particle and the reaction plane is defined by the telescope position and the beam axis.

The other competitive channels, fed by low-lying states in $^{20}Ne^*$ or $^{12}C^*$ have in principle equal chance to be emitted in any reaction plane defined by the total angular-momentum conservation law and by the geometry of the experimental set-up. Thus in order to enhance the contribution of the reaction under consideration and reduce the background due to the other two processes, the coplanarity condition between particles in the final state was imposed, that is, events involving ^{8}Be emission in the horizontal plane were selected.

The $^{16}O_{g.s.}$-$^{8}Be_{g.s.}$ relative-energy spectrum so obtained is shown in fig. 5b. Here, it is evident that the constraint of coplanarity allows for a better definition of the structures in fig. 5a, despite the lower statistics.

Dots in both spectra show the efficiency behaviour as a function of the $^{16}O_{g.s.}$-$^{8}Be_{g.s.}$ relative energy. The detection efficiency was calculated for each angle pair of the detected particles by means of a Monte Carlo simulation code. A sequential break-up process was assumed to populate the final three-body channel. The emission of fragments in the centre-of-mass frame was considered to be isotropic in both steps of the reaction. This assumption does not affect the efficiency calculations, which are only slightly sensitive to different shapes of angular distributions.

The spectrum in fig. 5b shows resonant structures with characteristic widths around 1 MeV, ranging between 20 and 38 MeV. These widths are affected by our experimental relative-energy resolution which has been evaluated to be about 250 keV. A set of peaks at 22.1, 26.3, (27.3), 28.5, (30.3) and 32.4 MeV can be associated with the resonances of the $^{12}C(^{12}C,{}^{8}Be_{g.s.})^{16}O_{g.s.}$ excitation function measured in the same range of ^{24}Mg excitation energy [9, 10].

For a further confirmation of the origin of the mentioned structures, a $^{16}O_{g.s.}$-$^{8}Be_{g.s.}$ relative-energy spectrum, gated on the final-state interaction region free from contaminant decays of ^{20}Ne, has been obtained and shown in fig. 5c. The structures are still present and even better evidenced, although the statistics is strongly reduced.

An angular-correlation analysis was performed in order to get information on the spin value of the observed resonances. Due to the low statistics, a meaningful analysis could be performed only for the peaks marked by arrows in fig. 5b.

Following the procedure of refs. [17,18], $^{8}Be_{g.s.}$-$^{16}O_{g.s.}$ coincidence events must be reported in the (θ^*,Ψ)-plane, θ^* and Ψ being the centre-of-mass angle of the emitting $^{24}Mg^*$ and the angle between the beam axis and the direction of $^{8}Be_{g.s.}$ and $^{16}O_{g.s.}$ emission in the $^{24}Mg^*$ frame, respectively. If a spin value is dominant in the decay process, then the events are expected to fall on ridges whose slope, which is constant close to the $\theta^* = 0$ region, is related to the spin of the decaying system.

Figure 6a shows an example of θ^*-Ψ angular-correlation matrix obtained by gating on the 34.5 MeV structure in the $^{16}O_{g.s.}$-$^{8}Be_{g.s.}$ relative-energy spectrum. Figure 6b shows the corresponding correlation matrix calculated by means of a Monte Carlo simulation code. The

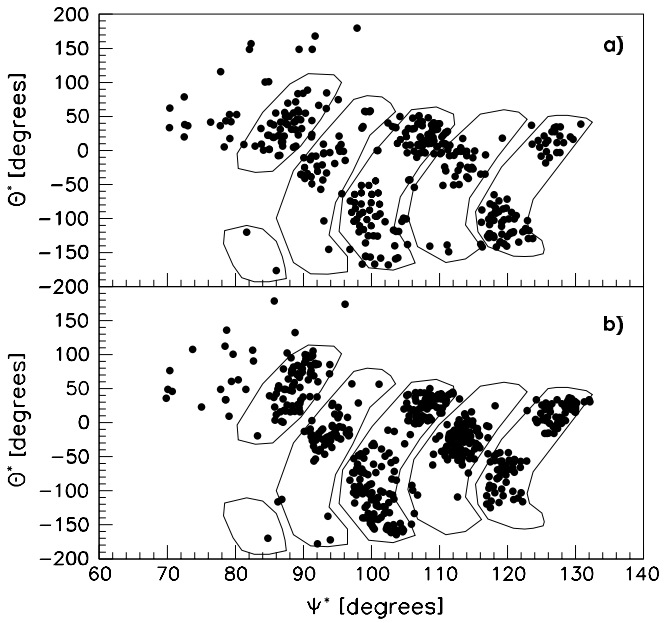

Fig. 6. The θ^*-Ψ angular correlation for the 48.6 MeV state of ^{24}Mg. Data are reported in a), while b) shows the results of a Monte Carlo calculation. The full lines in both spectra represent the calculated correlation matrix in the ideal case of no dead angular regions between ASPEDs.

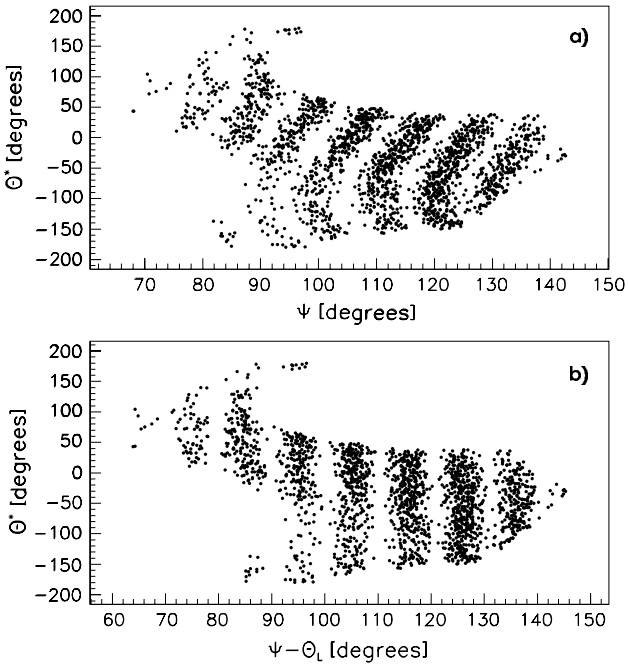

Fig. 7. a) θ^* *vs.* Ψ and b) θ^* *vs.* Ψ' correlation diagrams, referring to the 34.5 MeV structure of the $^{16}O_{g.s.}$-$^{8}Be_{g.s.}$ relative-energy spectrum and calculated under the same geometrical conditions as for the full lines of fig. 6.

calculation was performed accounting for the same sensitivity and performance of the detection system. A break-up process of ^{24}Mg* was assumed to take place from a level with a given intrinsic spin J ($J = 17$ in the figure). The contour lines drawn in both spectra refer to the same calculation performed under the hypothesis that the four ASPEDs are fused together into a single one covering the total experimental polar angular range (20°–60°). These lines allow for a clear understanding of the ridge behaviour otherwise strongly affected because of the dead angular regions between the ASPEDs.

A fair agreement shows up between the experimental θ^*-Ψ matrix and the calculated one, although the statistics is low. Distortion effects from the linear θ^*-Ψ relation are also visible at large θ^* angles, as already predicted in ref. [18].

As known from refs. [17,18], the angular correlation is obtained after projection of the data onto the $\theta^* = 0$ axis along the slope of the ridges. The periodicity of such correlation is expected to follow that of a Legendre polynomial of order J, the dominant spin value of ^{24}Mg*. Unfortunately, the projection procedure is difficult to implement at large θ^* angles, due to the already mentioned distortion effects from the linear slope.

However, in special cases when the direction of the emitting nucleus is a symmetry axis for the correlation function, an alternative way to obtain the information on the spin J can be used [17]. The correlation function is thus expressed in a simplified form, which does not depend any more on both θ^* and Ψ angles, but is proportional to a Legendre polynomial with argument $\Psi' = \Psi - \theta_L$, being θ_L the angle of the emitting ^{24}Mg* in the laboratory system [17]. The angular distribution of this new angle simply carries out the required information on J in a way which avoids the problem of the θ^*-Ψ locus distortion allowing for using all the available data to carry out the information on the spin.

Indeed, due to the coplanarity constraint imposed to our reaction products, the ^{24}Mg direction of emission turns out to be a symmetry axis for the system under study, thus justifying the use of the simplified correlation function.

Angular distributions were then calculated as a function of Ψ' by means of the Monte Carlo simulation code. The two angles, θ^* and Ψ', were extracted independently in order to fulfil the symmetry requirement for which a lack of correlation between them is expected. This produces the appearance of vertical ridges in the θ^* *vs.* Ψ' plot whose periodicity again reflects that of the Legendre polynomial of order J. For clearness, it is worth showing both correlation diagrams, θ^* *vs.* Ψ (fig. 7a) and θ^* *vs.* Ψ' (fig. 7b), referring to the 34.5 MeV structure of the $^{16}O_{g.s.}$-$^{8}Be_{g.s.}$ relative-energy spectrum and calculated under the same geometrical conditions as for the contour lines of fig. 6.

Examples of angular distributions obtained from the data are reported in figs. 8 to 10 together with the calculations performed assuming intrinsic spin values for ^{24}Mg* of $J-2$, J and $J+2$, J being the spin value which can be expected in the excitation energy range of the resonance.

Despite the low statistics, the reasonable agreement between data and calculations makes us quite confident on the validity of the approximation used. A dominant

Table 1. Energy-spin systematic for the structures of fig. 5b. Row (a) reports on the spin presently estimated by means of angular-correlation measurements within an uncertainty $\delta J = \pm 2$; row (b) refers to the analysis of refs. [9,10]; row (c) reports spin values calculated by means of the rotational expression of refs. [9,10].

				$^{24}\mathrm{Mg} \rightarrow$		$^{16}\mathrm{O_{g.s.}} + {}^{8}\mathrm{Be_{g.s.}}$			
$E^*(^{24}\mathrm{Mg})$ (MeV)	36.2	40.4	41.4	42.6	44.4	46.4	47.4	48.6	50.9
(a) $J(\delta J = \pm 2)$	10^+			12^+		14^+–16^+	14^+	17^-	18^+
(b) J	12^+	(16^+)	14^+	14^+		16^+			
(c) J from fit	12.8	14.4	14.7	15.1	15.8	16.4	16.7	17.1	17.8

spin value can then be associated to each resonance, by recognising the calculated oscillatory pattern that better reproduces the experimental periodicity. Because of the strong absorbing character of heavy-ion reactions at these energies, one expects that the reaction under consideration is mostly peripheral. Hence, the experimental periodicity should reflect a Legendre pattern with l-value close to l_{graz}. However, it has been shown by several authors [19, 20] that, in order to fit the full shape of such kinds of angular distributions, a coherent contribution of several partial waves is needed. Moreover, due to high-level density in this excitation energy region, states with different spins may be expected to overlap in the same structure. This appears to be the case also here, and local distortions from a single Legendre polynomial pattern can be seen from the data. Nevertheless it is possible to give an estimation of the dominant J-value within an uncertainty of $\pm 2\hbar$.

4 Discussion and conclusions

In table 1 the results of the present experiment are summarised and compared with the data of refs. [9,10]. Row (a) reports on the dominant spin assignment carried out in the present angular-correlation measurement; row (b) refers to the spin analysis reported in refs. [9,10]; row (c) reports the spin values calculated by means of the expression $E_{^{16}\mathrm{O}\text{-}^{8}\mathrm{Be}} = 5.6 + 0.093J(J+1)$ [9,10], which results from the fit of data of refs. [6,18,21–24] and whose slope fairly agrees with that of the $D1$ rotational band.

There is a nice similarity between the two sets of data, as far as even-spin states are concerned. Among these, the 46.4 MeV resonance also shows up in the present data, which has been so far observed only in a number of exit channels of the $^{12}\mathrm{C} + {}^{12}\mathrm{C}$ interaction and whose nature has been the object of a wide debate.

Different models based on either the "strong-coupling approach" (Shape Eigenstate Model) [25] or the "weak-coupling approach" (Band Crossing Model) [26,27] succeeded in satisfactorily justifying the overall characteristics of this resonance. Thus they left unsolved the question of whether it is meaningful the association with a local minimum in the Nilsson potential energy surface or on the contrary the resonance simply represents a manifestation of entrance channel effects, as explained for example in the BCM frame in terms of the effective increase of the moment of inertia due to the "spin alignment" mechanism [26–28].

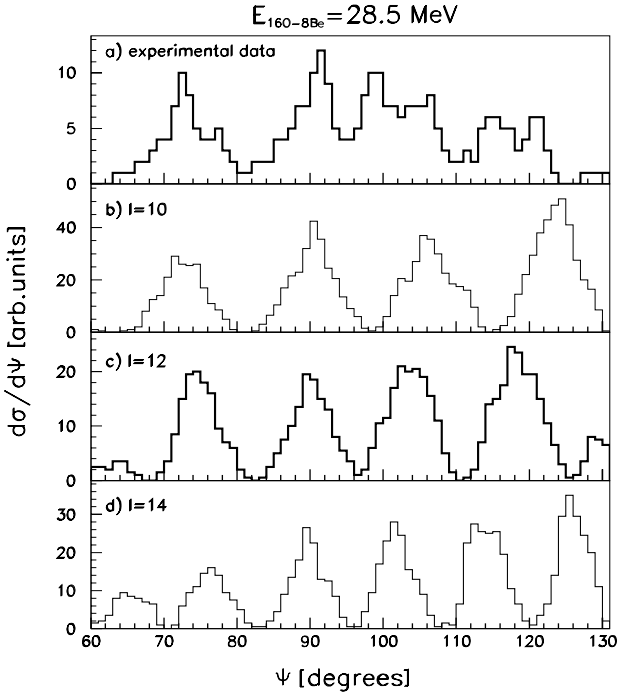

Fig. 8. a) Ψ' experimental angular distributions for the $E_{^{16}\mathrm{O}\text{-}^{8}\mathrm{Be}} = 28.5$ MeV structure; data periodicity is compared with that of the calculation assuming in turn b) $J = 10$, c) $J = 12$ and d) $J = 14$ for the emitting ^{24}Mg nucleus.

Recently, a more complete and successful calculation on the experimental $^{12}\mathrm{C} + {}^{12}\mathrm{C}$ elastic and inelastic resonances has been performed in the frame of the coupled-channel approach. The calculation makes use of a more realistic nucleon-nucleon potential based on the multipole expansion of the nucleon densities [28]. The addition of the higher multipole part of the densities appears to significantly modify the BCM rotational bands, resulting in a stronger channel coupling effect which indicates a more complex reaction dynamics than that of the weak-coupling picture.

The present observation of the same resonant structure through indirect break-up of ^{24}Mg points to the "strong-coupling" interpretation, supporting the idea of existence of shape eigenstates. Indeed, the appearance of the same

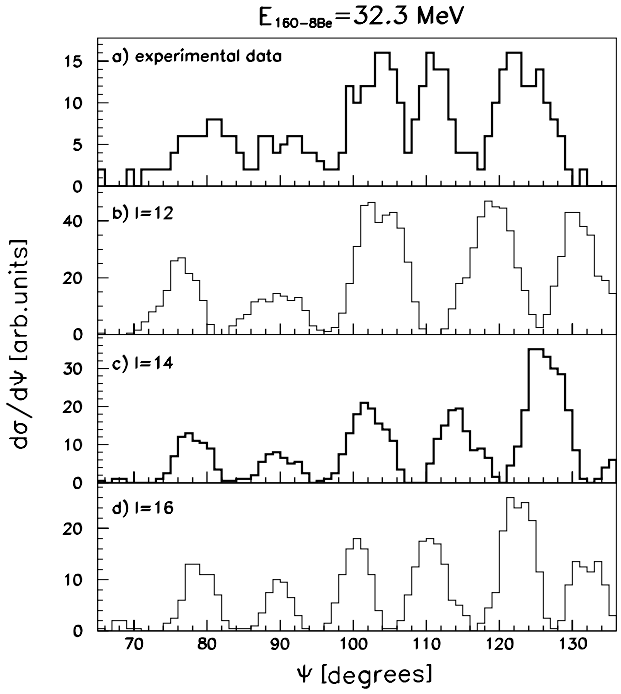

Fig. 9. a) Ψ' experimental angular distributions for the $E_{^{16}\mathrm{O}\text{-}^{8}\mathrm{Be}} = 32.3$ MeV structure; data periodicity is compared with that of the calculation assuming in turn b) $J = 12$, c) $J = 14$ and d) $J = 16$ for the emitting ^{24}Mg nucleus.

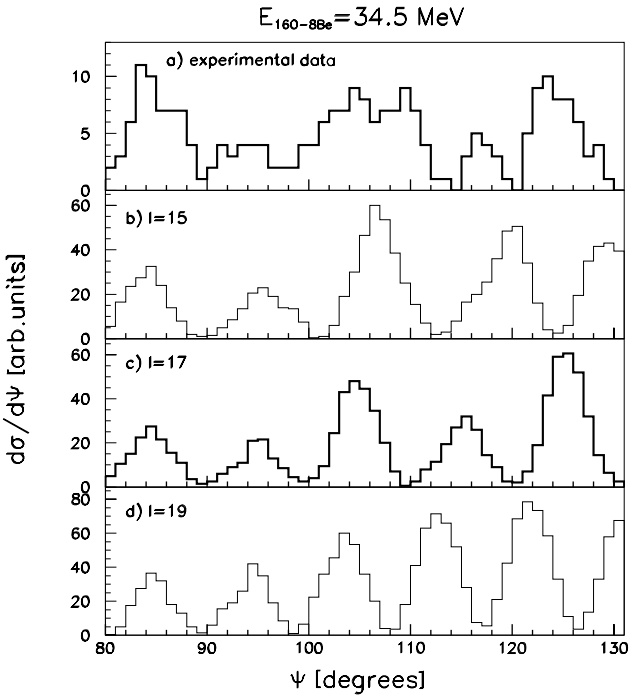

Fig. 10. a) Ψ' experimental angular distributions for the $E_{^{16}\mathrm{O}\text{-}^{8}\mathrm{Be}} = 34.5$ MeV structure; data periodicity is compared with that of the calculation assuming in turn b) $J = 15$, c) $J = 17$ and d) $J = 19$ for the emitting ^{24}Mg nucleus.

resonance in ^{24}Mg produced through different reaction mechanisms should indicate the effect of structural properties rather than that of the entrance channel potential.

The structure in ^{24}Mg excitation spectrum extends to higher energies never investigated up to now through the $^{16}\mathrm{O}_{\mathrm{g.s.}} + {}^{8}\mathrm{Be}_{\mathrm{g.s.}}$ decay channel, revealing the presence of further well-defined resonances at relative energy of 33.3, 34.5 and 36.8 MeV, respectively. The 33.3 MeV structure, which was observed in other decay channels, could not be resolved in the $^{12}\mathrm{C}(^{12}\mathrm{C},{}^{8}\mathrm{Be}_{\mathrm{g.s.}})^{16}\mathrm{O}_{\mathrm{g.s.}}$ excitation function we studied up to 36 MeV [9,10], due to the large energy step in that region (see fig. 3 of ref. [10]). The lack of evidence for the 34.5 MeV resonance in the same experiment might be connected with the symmetry of the $^{12}\mathrm{C} + {}^{12}\mathrm{C}$ entrance channel which selects even-spin and positive-parity states, thus preventing any odd-spin state to be populated. This is consistent with the odd-spin assignment to the 34.5 MeV resonance, whose angular-distribution periodicity resembles that of a Legendre polynomial of order 17 (see fig. 9).

Energies and spins for these new resonances still follow the same rotational rule of the ones at lower energies, suggesting the association of the same $^{16}\mathrm{O}_{\mathrm{g.s.}}-2\alpha$ configuration to all of them. Because of the even symmetry of the $^{16}\mathrm{O}_{\mathrm{g.s.}}-2\alpha$ configuration, odd-spin states are not allowed to belong to its rotational band. However, stretching and bending vibrations are expected to exist for this configuration. Indeed the 34.5 MeV resonance, to which an odd-spin value was associated, might represent an additional evidence for bending vibrations in the $^{16}\mathrm{O}_{\mathrm{g.s.}}-2\alpha$ system, and the first one at so high excitation energy.

It is to be pointed out that the angular momentum measured for these resonances represents the limit value predicted by Cranked Cluster Model calculations [12], beyond which the $^{16}\mathrm{O}_{\mathrm{g.s.}}-2\alpha$ configuration should not exist.

We would like to thank prof. F. Iachello for the enlightening and fruitful discussions. We are indebted to the technical staff of LNS, in particular to C. Calì, P. Litrico, S. Marino and F. Ferrera, for the effective assistance during the experiment.

References

1. A.H. Wuosmaa, R.R. Bets, B.B. Back, M. Freer, B.G. Glagola, Th. Happ, D.J. Henderson, P. Wilt, I.G. Bearden, Phys. Rev. Lett. **68**, 1295 (1992).
2. S.P.G. Chappell, D.L. Watson, S.P. Fox, C.D. Jones, W.D.M. Rae, P.M. Simmons, M. Freer, B.R. Fulton, N.M. Clarke, N. Curtis, M.J. Leddy, J.S. Pople, S.J. Hall, R.P. Ward, G. Tungate, W.N. Catford, G.J. Gyapong, S.M. Singer, P.H. Regan, Phys. Rev. C **51**, 695 (1995).
3. R.M. Freeman, F. Haas, A. Elanique, A. Morsad, C. Beck, Phys. Rev. C **51**, 3504 (1995).
4. S. Szilner, Z.Basrak, R.M. Freeman, F. Haas, A. Morsad, C. Beck, Phys. Rev. C **55**, 1312 (1997).
5. M. Aliotta, S.Cherubini, E. Costanzo, M. Lattuada, S. Romano, D. Vinciguerra, M. Zadro, Z. Phys. A **353**, 43 (1995).
6. M. Aliotta, S. Cherubini, E. Costanzo, M. Lattuada, S. Romano, C. Spitaleri, A. Tumino, D. Vinciguerra, M. Zadro, Z. Phys. A **354**, 119 (1996).

7. R.A. Le Marechal, N.M. Clarke, M. Freer, B.R. Fulton, S.J. Hall, S.J. Hoad, G.R. Kelly, R.P. Ward, C.D. Jones, P. Lee, D.L. Watson, Phys. Rev. C **55**, 1881 (1997).
8. E.T. Mirgule, M.A. Eswaran, S. Kumar, D.R. Chakrabarty, V.M. Datar, U.K. Pal, H.H. Oza, N.L. Ragoowansi, Phys. Rev. C **56**, 1943 (1997).
9. S. Cherubini, E. Costanzo, A. Cunsolo, A. Foti, M. Lattuada, S. Romano, C. Spitaleri, A. Tumino, D. Vinciguerra, M. Zadro, Z. Phys. A **357**, 291 (1997).
10. M. Lattuada, E. Costanzo, A. Cunsolo, A. Foti, S. Romano, C. Spitaleri, A. Tumino, D. Vinciguerra, M. Zadro, Nuovo Cimento A **110**, 1007 (1997).
11. S. Marsh, W.D.M. Rae, Phys. Lett. B **180**, 185 (1986).
12. M. Freer, N.M. Clarke, B.R. Fulton, J.T. Murgatroyd, A.S.J. Murphy, Phys. Rev. C **57**, 1277 (1998).
13. N. Randazzo, G.V. Russo, C. Caligiore, D. Lo Presti, C. Petta, S. Reito, L. Todaro, G. Fallica, G. Valvo, M. Lattuada, S. Romano, A. Tumino, IEEE Trans. Nucl. Sci. **46**, 1300 (1999).
14. A. Tumino, Ph.D. Thesis, Università di Catania (2000).
15. S.C. Allcock, W.D. Rae, P.R. Keeling, A.E. Smithm B.R. Fulton, D.W. Banes, Phys. Lett. B **201**, 201 (1988).
16. G.R. Kelly, N.M. Clarke, M.Freer, B.R. Fulton, S.J. Haod, R.A. Le Marechal, R.P. Ward, Nucl. Phys. A **628**, 62 (1998).
17. E.F. da Silveira, *Contribution to the XIV Winter Meeting on Nuclear Physics, Bormio 1976*, edited by I. Iori (Physics Department, University of Milano) p. 293.
18. M. Freer, Nucl. Instrum. Methods Phys. Res. A **383**, 463 (1996).
19. W.D.M. Rae, A.C. Merchant, B. Buck. Phys. Rev. Lett. **69**, 3709 (1992).
20. R.M. Freeman, F. Haas, M.P. Nicoli, A. Morsad, Z. Basrak, Eur. Phys. J. A **4**, 239 (1999).
21. R. Wada, T. Murakami, E. Takada, M. Fukada, K. Takimodo, Phys. Rev. C **22**, 557 (1980).
22. D.R. James, N.R. Fletscher, Phys. Rev. C **17**, 2248 (1978).
23. K. Eberhard, A. Mathiak, E. Stettmeir, J.W. Trombik, A. Weidinger, L.N. Wuestefeld, K.G. Bernhardt, Phys. Lett. B **56**, 445 (1975).
24. W.D.M. Rae, P.R. Keeling, Nucl. Phys. A **575**, 207 (1994).
25. W.D.M. Rae, A.C. Merchant, *Proceeding of the International Conference on Clusters in Nuclear Structure and Dynamics, Strasbourg, France, 1994*, edited by F. Haas (Centre de Recherches Nucléaires) p. 39.
26. Y. Abe, Y. Kondo, T. Matsuse, Prog. Theor. Phys. **68**, 303 (1980).
27. Y. Hirabayashi, Y. Sakuragi, Y. Abe, Phys. Rev. Lett. **74**, 4141 (1995).
28. M. Ito, Y. Sakuragi, Y. Hirabayashi, Phys. Rev. C **63**, 064303 (2001).